Observation and Analysis of High-energy Gamma-rays observed with CALET on the ISS

国際宇宙ステーション搭載CALETによるガンマ線の観測と解析

立命館大理工, 早大理工研[A],
NASA/GSFC[B], Louisiana State Univ.[C],

森正樹, 赤池陽水[A], 小林兼好[A], 鳥居祥二[A],
N. Cannady[B], 川久保雄太[C], M.L. Cherry[C],
他CALETチーム

M. Mori, Y. Akaike, K. Kobayashi, S. Torii, N. Cannady, Y. Kawakubo, M.L. Cherry for the CALET collaboration

第22回宇宙科学シンポジウム（オンライン開催）2022年1月6～7日

See also PoS (ICRC2021) 619

The CALET collaboration

O. Adriani[1,2], Y. Akaike[3,4], K. Asano[5], Y. Asaoka[5], E. Berti[1,2], G. Bigongiari[6,7], W.R. Binns[8], M. Bongi[1,2], P. Brogi[6,7], A. Bruno[9.10], J.H. Buckley[8], N. Cannady[11,12,13], G. Castellini[14], C. Checchia[6],M.L. Cherry[15], G. Collazuol[16,17], K. Ebisawa[18], A.W. Ficklin[15], H. Fuke[18], S. Gonzi[1,2], T.G. Guzik[15], T. Hams[11], K. Hibino[19], M. Ichimura[20], K. Ioka[21], W. Ishizaki[5], M.H. Israel[8], K. Kasahara[22], J. Kataoka[23], R. Kataoka[24], Y. Katayose[25], C. Kato[26], N. Kawanaka[27,28], Y. Kawakubo[15], K. Kobayashi[3,4],K. Kohri [29], H.S. Krawczynski[8], J.F. Krizmanic[11,12,13], J. Link[11,12,13], P. Maestro[6,7], P.S. Marrocchesi[6,7], A.M. Messineo[30,7], J.W. Mitchell[31], S. Miyake[32], A.A. Moiseev[33,12,13], M. Mori[34], N. Mori[2], H.M. Motz[35], K. Munakata[26], S. Nakahira[18], J. Nishimura[18], G.A. de Nolfo[9], S. Okuno[19], J.F. Ormes[36], N. Ospina[16,17], S. Ozawa[37], L. Pacini[1,14,2], P. Papini[2], B.F. Rauch[8], S.B. Ricciarini[14,2], K. Sakai[11,12,13], T. Sakamoto[38], M. Sasaki[32,12,13], Y. Shimizu[19], A. Shiomi[39], P. Spillantini[1], F. Stolzi[6,7], S. Sugita[38], A. Sulaj[6,7], M. Takita[5], T. Tamura[19], T. Terasawa[40], S. Torii[3], Y. Tsunesada[41], Y. Uchihori[42], E. Vannuccini[2], J.P. Wefel[15], K. Yamaoka[43], S. Yanagita[44], A. Yoshida[38], K. Yoshida[22], and W.V. Zober[15]

1) University of Florence, Italy
2) INFN Florence, Italy
3) RISE, Waseda University, Japan
4) JEM Utilization Center, JAXA, Japan
5) ICRR, University of Tokyo, Japan
6) University of Siena, Italy
7) INFN Pisa, Italy
8) Washington University, St. Louis, USA
9) Heliospheric Physics Lab., NASA/GSFC, USA
10) Catholic University of America, Washington DC, USA
11) University of Maryland, USA
12) Astroparticle Physics Lab., NASA/GSFC, USA
13) CRESST, NASA/GSFC, USA
14) IFAC, CNR, Fiorentino, Italy
15) Louisiana State University, USA
16) University of Padova, Italy
17) INFN Padova, Italy
18) ISAS, JAXA, Japan
19) Kanagawa University, Japan
20) Hirosaki University, Japan
21) YITP, Kyoto University, Japan
22) Shibaura Institute of Technology, Japan
23) Waseda University, Japan
24) National Institute of Polar Research, Japan
25) Yokohama National University, Japan
26) Shinshu University, Japan
27) Hakubi Center, Kyoto University, Japan
28) Kyoto University, Japan
29) IPNS, KEK, Japan
30) University of Pisa, Italy
31) National Institute of Technology, Japan
33) University of Maryland, USA
34) Ritsumeikan University, Japan
35) GCSE, Waseda University, Japan
36) University of Denver, USA
37) National Institute of Information and Communications Technology, Japan
38) Aoyama Gakuin University
39) Nihon University, Japan
40) RIKEN, Japan
41) Osaka City Univiersity, Japan
42) National Institutes for Quantum and Radiation Science and Technology, Japan
43) Nagoya University, Japan
44) Ibaraki University, Japan

See Poster: Torii et al. for summary of CALET results

CALET/CAL Detector

Fully active thick calorimeter (30 radiation lengths [X_0]) optimized for electron spectrum measurements well into TeV region

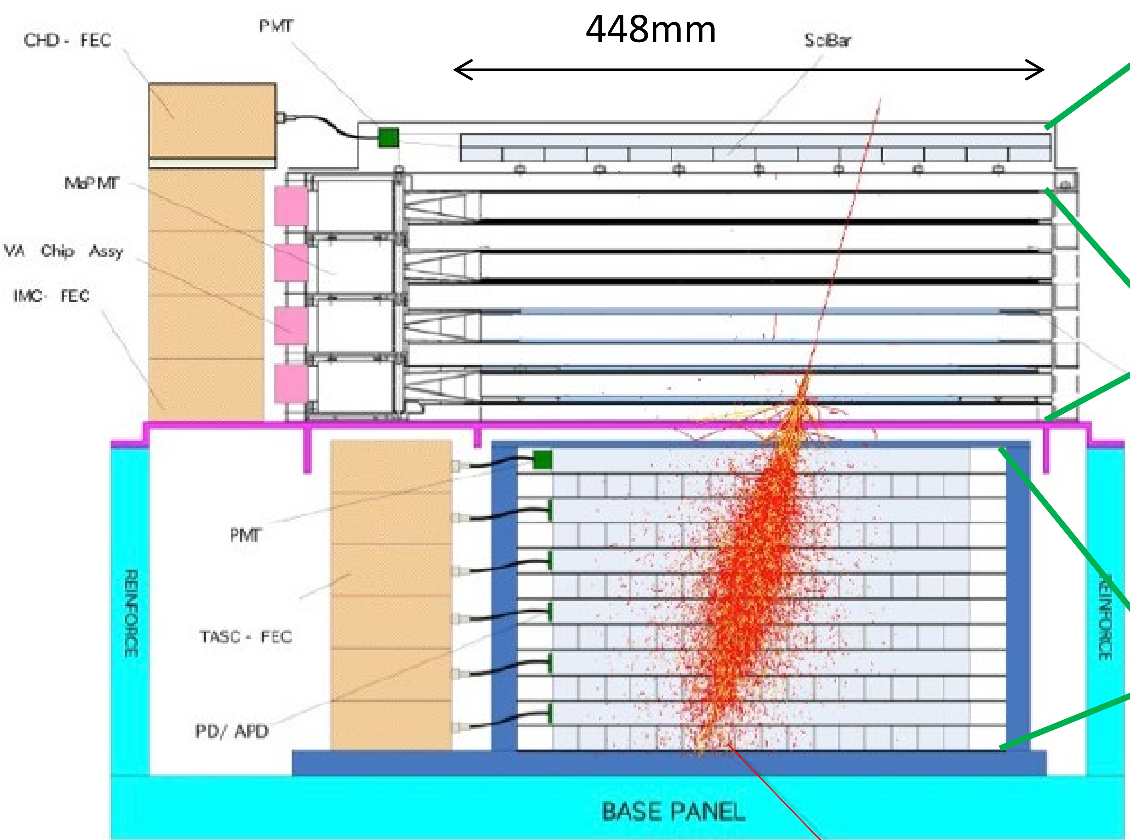

1 TeV electron shower is fully contained in TASC

Charge Detector **CHD**

plastic scintillator hodoscope, absolute charge measurement (including charge zero)

Imaging Calorimeter **IMC**

SciFi + tungsten plate (3X_0), reconstruction of arrival direction and initial shower development

Total Absorption Calorimeter **TASC**

PWO hodoscope (27X_0), energy measurements and particle identification

See Poster: Kawakubo et al. for CALET/CGBM results

Cannady et al., ApJS 238:5 (2018)

Gamma Ray Event Selection

= Electron Selection Cut + Gamma-ray ID Cut w/ Lower Energy Extension

100 GeV Event Examples

gamma-ray | electron | proton

Charge Z=0 | Charge Z=1

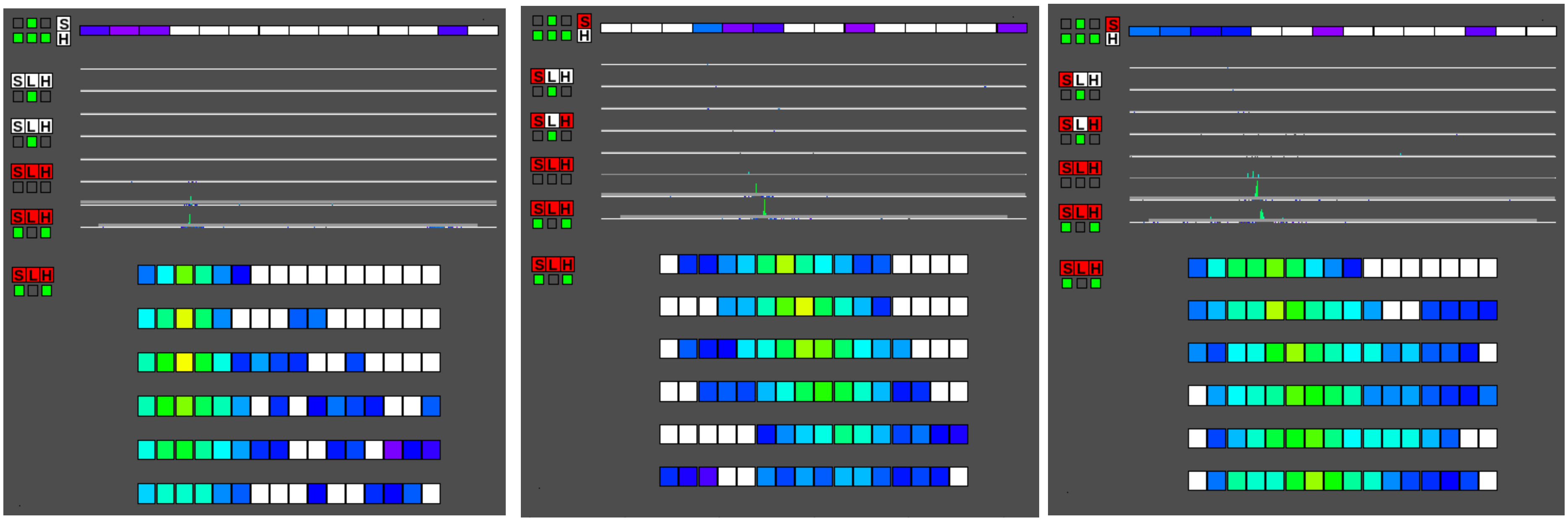

Electromagnetic Shower | Hadron Shower

well contained, regular shower development | larger spread

CALET performance for HE trigger

- HE trigger (>10 GeV) is always active in normal observations
- LE-γ trigger (>1 GeV) mode is activated when the geomagnetic latitude is below 20° or following a CALET Gamma-ray Burst Monitor (CGBM) burst trigger

Energy resolution

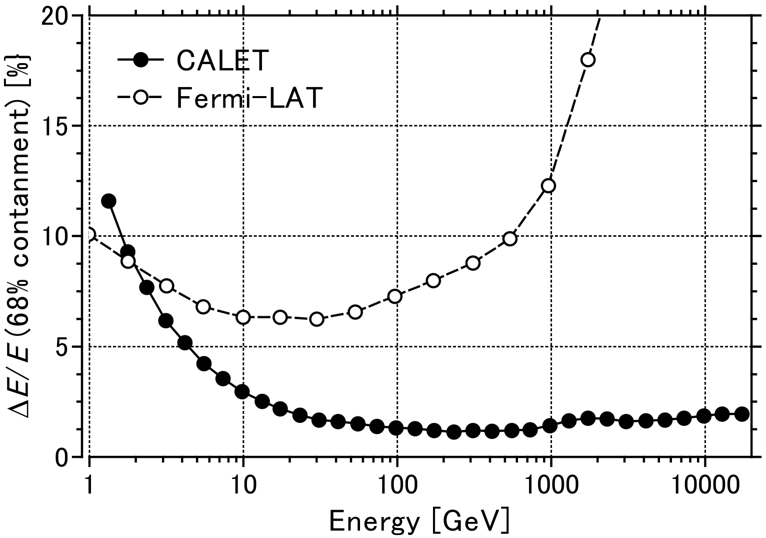

Asaoka et al, Astropart. Phys. 91, 1 (2017)

Effective area (for gamma rays)

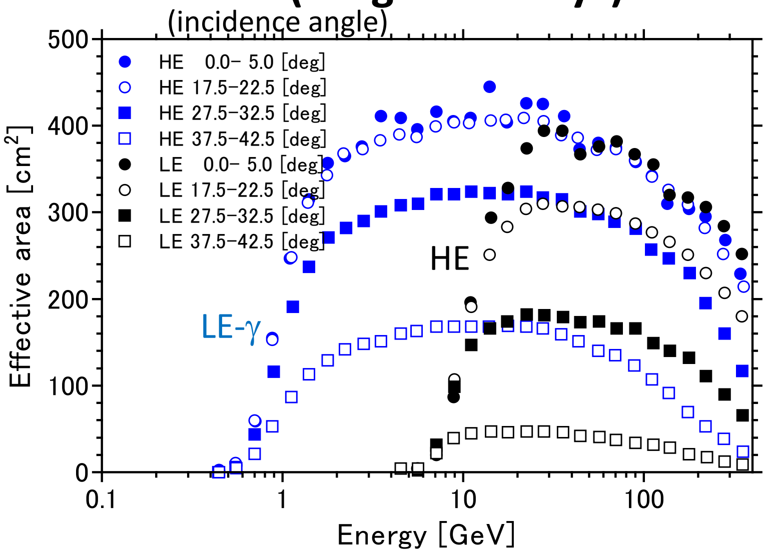

Cannady et al., ApJS 238, 5 (2018)

- Good energy resolution at high energies thanks to the thick calorimeter!

Skymap (LE-γ trigger, >1 GeV)

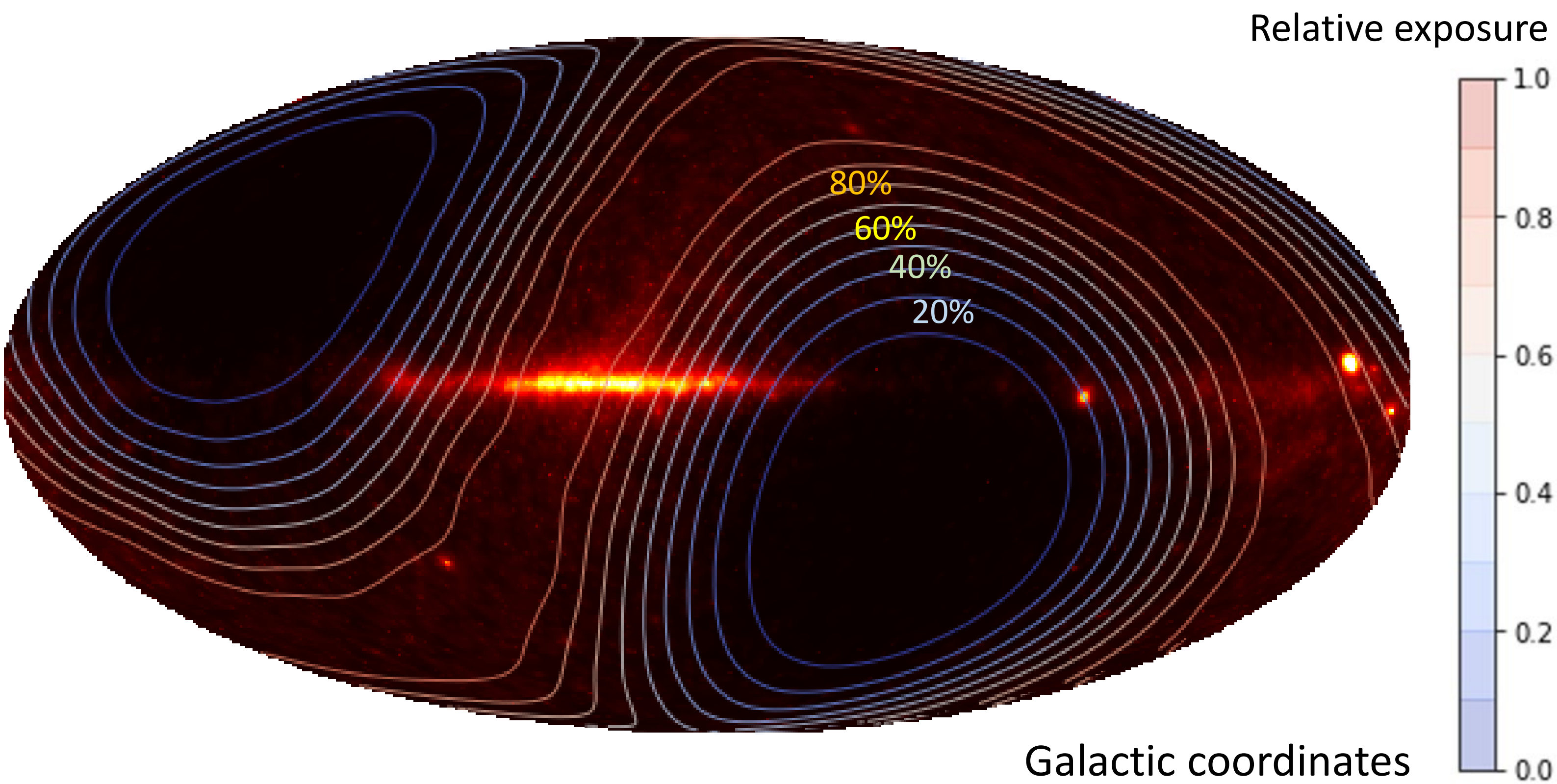

- Exposure is not uniform due to the ISS orbit (inclination 51.6°)

Point sources (LE-γ trigger, >1 GeV)

Preliminary

October 13, 2015 – September 30, 2020

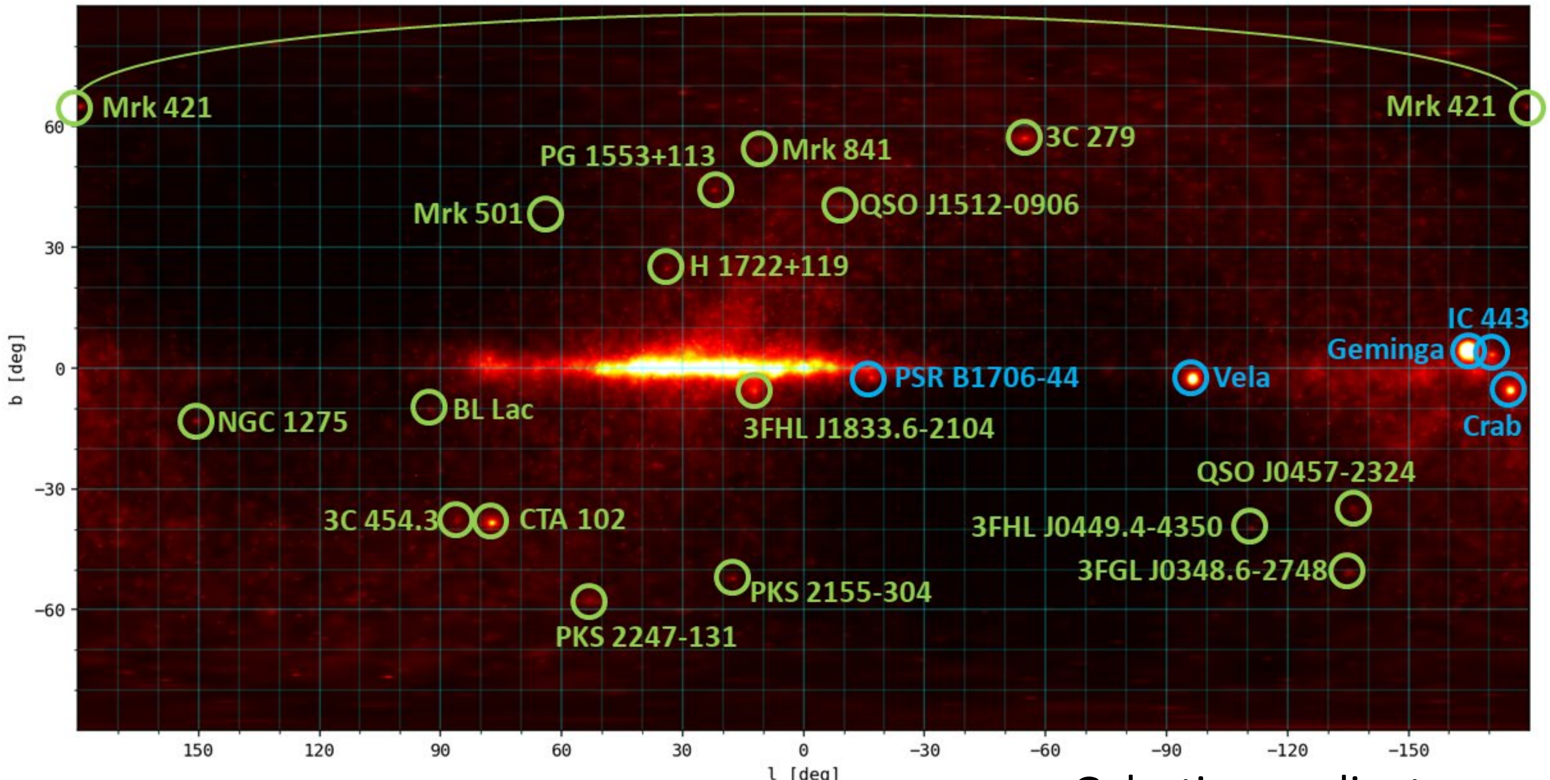

Galactic coordinates

- >20 point sources (Crab, Geminga, Vela, CTA102,…) have been detected.

See poster 322 (Cannady et al.) for LE-γ results

Skymap (HE trigger, >10 GeV)

Preliminary

October 13, 2015 – September 30, 2020
110,855 gamma-ray candidates

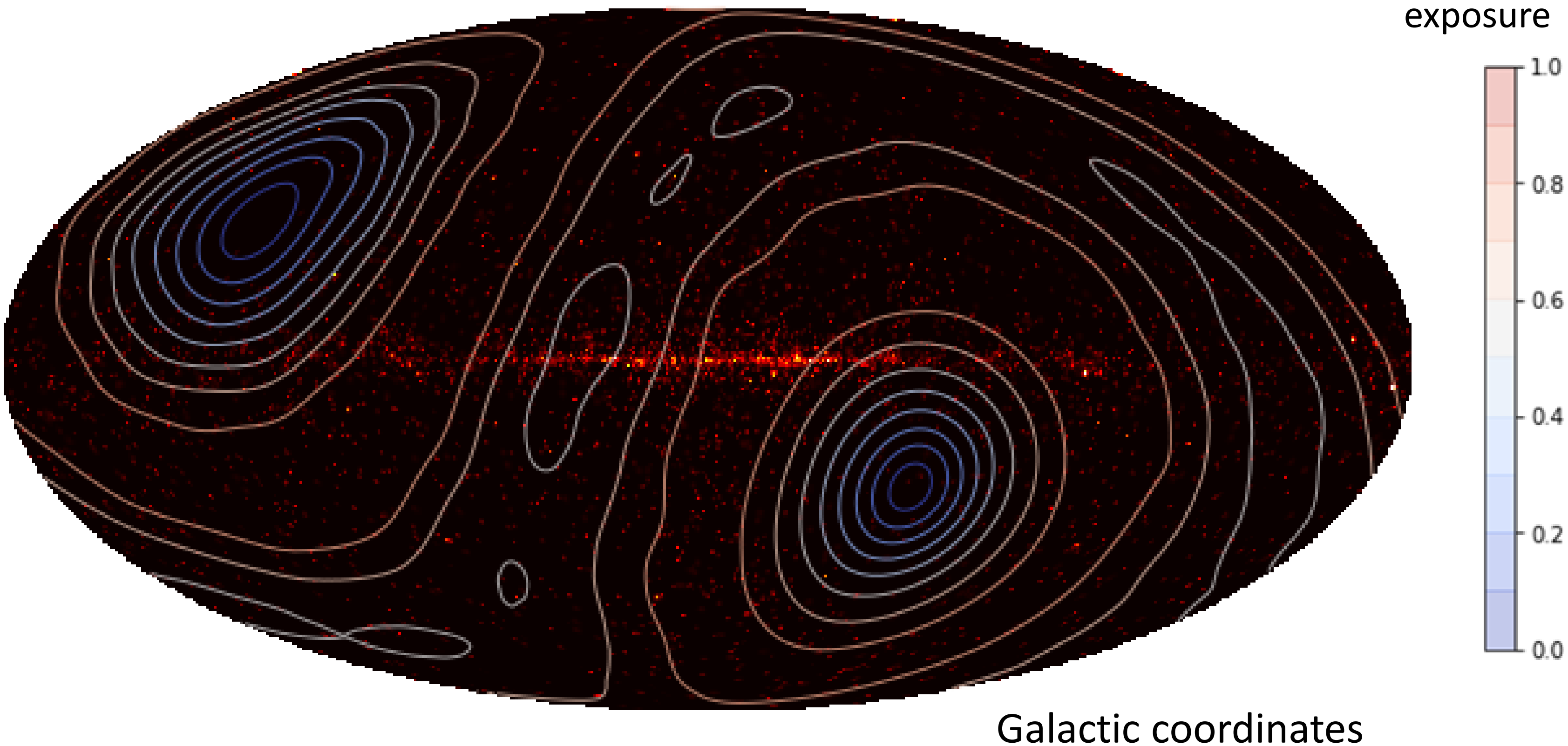

- Exposure is not uniform due to the ISS orbit (inclination 51.6°)

Gamma-ray spectra (LE-γ & HE)

Preliminary

October 13, 2015 – September 30, 2020

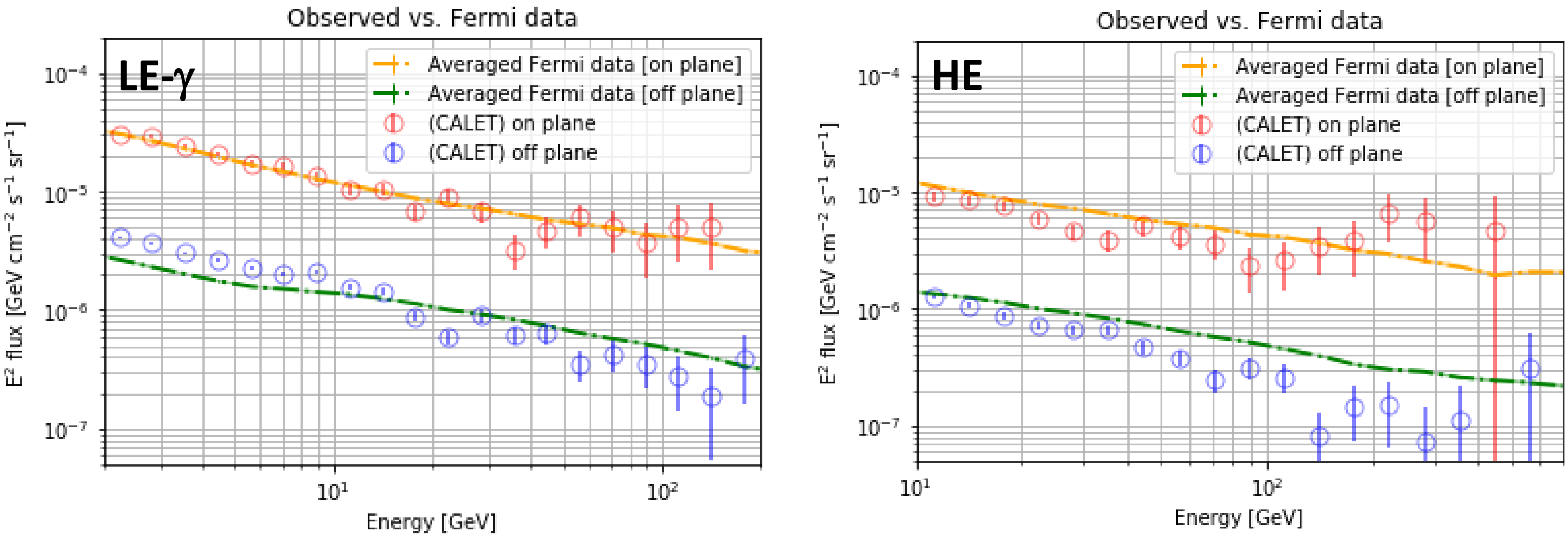

"**On-plane**": $|l| < 80°$ & $|b| < 8°$, "**Off-plane**": $|b| > 8°$

- The spectra (Galactic diffuse + point sources) look fairly consistent with those by Fermi-LAT.

Line signals from dark matter interaction

Annihilation: $\chi\,\chi \rightarrow \gamma\,\gamma$ etc., $E_\gamma = m_\chi$

T. Bringmann, C. Weniger / Dark Universe 1 (2012) 194–217

Note that generally the branching ratio into $\gamma\gamma$ suffers suppression ($< 10^{-3}$).

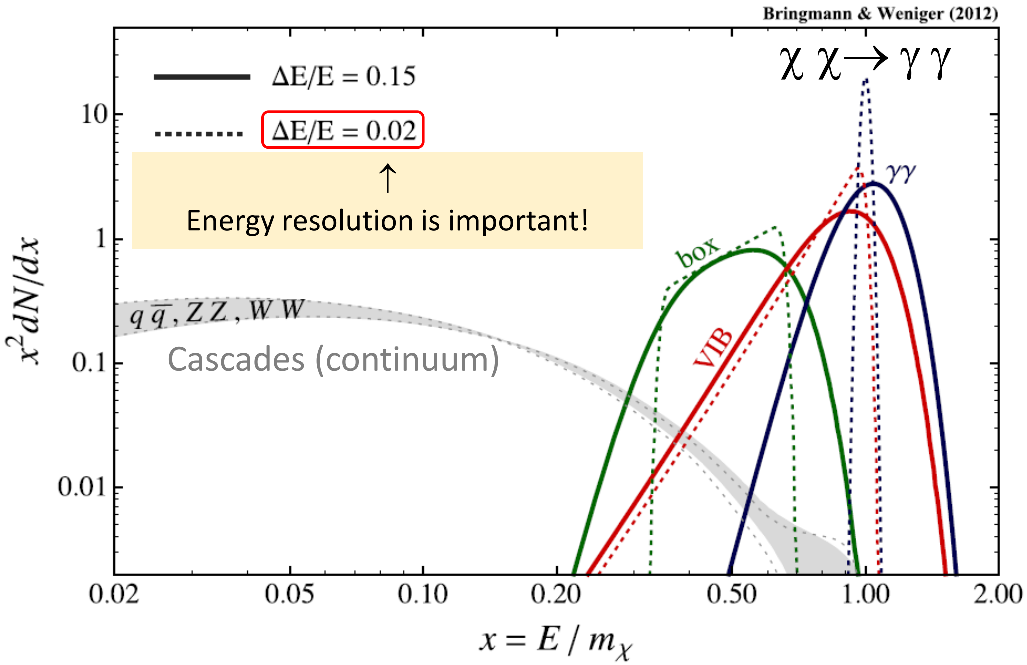

VIB (Virtual internal bremsstrahlung)

Decay: $\chi \rightarrow \gamma\,\nu$ etc., $E_\gamma = m_\chi/2$

Ibarra and Tran, PRL 100, 061301 (2008)

Dark matter distribution

- Dark matter halo is associated with our Galaxy and distributes spherically.
- Typical velocity: $v \sim O(10^{-3})c$

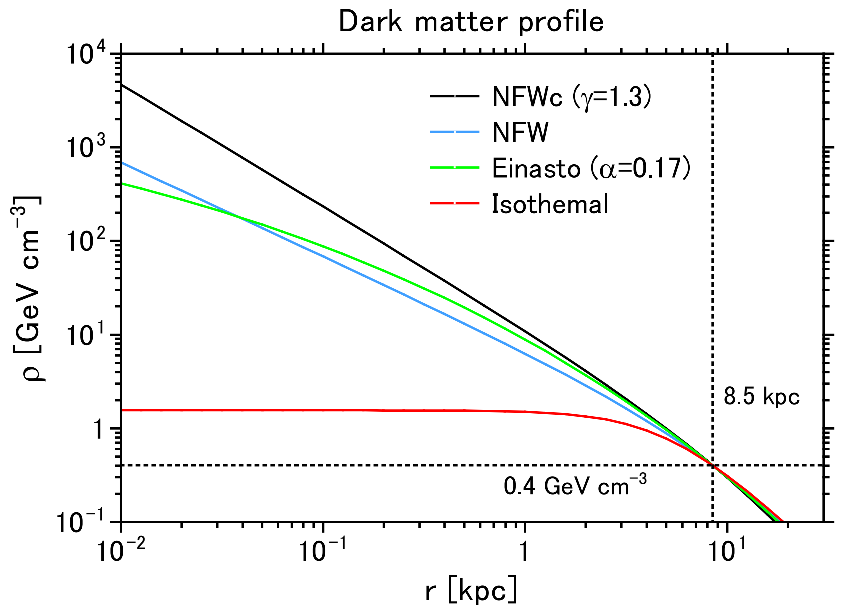

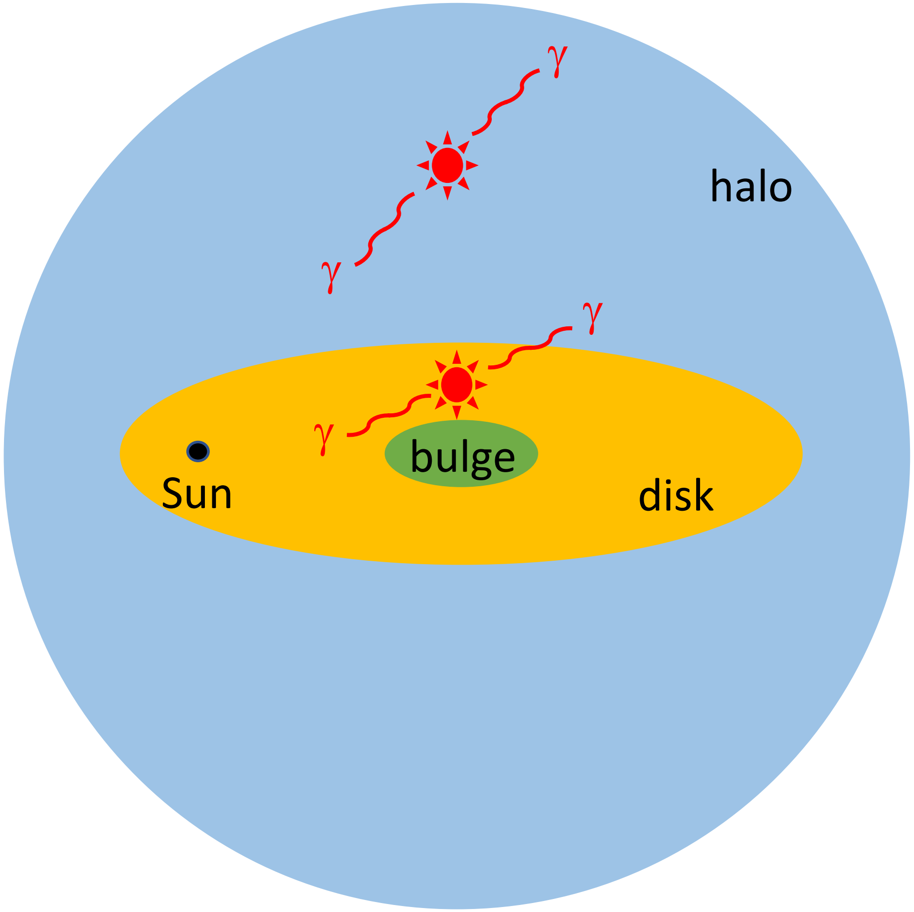

Profile is highly model dependent…

→ 4 models are assumed here.

Ref. Ackermann+, PR D91, 122002 (2015)

Ref. Ackermann+, PR D91, 122002 (2015)

Regions of interest (ROI)

R (angular distance from GC)
- <3° (NFWc profile)
- <16° (Einasto profile)
- <41° (NFW profile)
- <90° (isothermal)

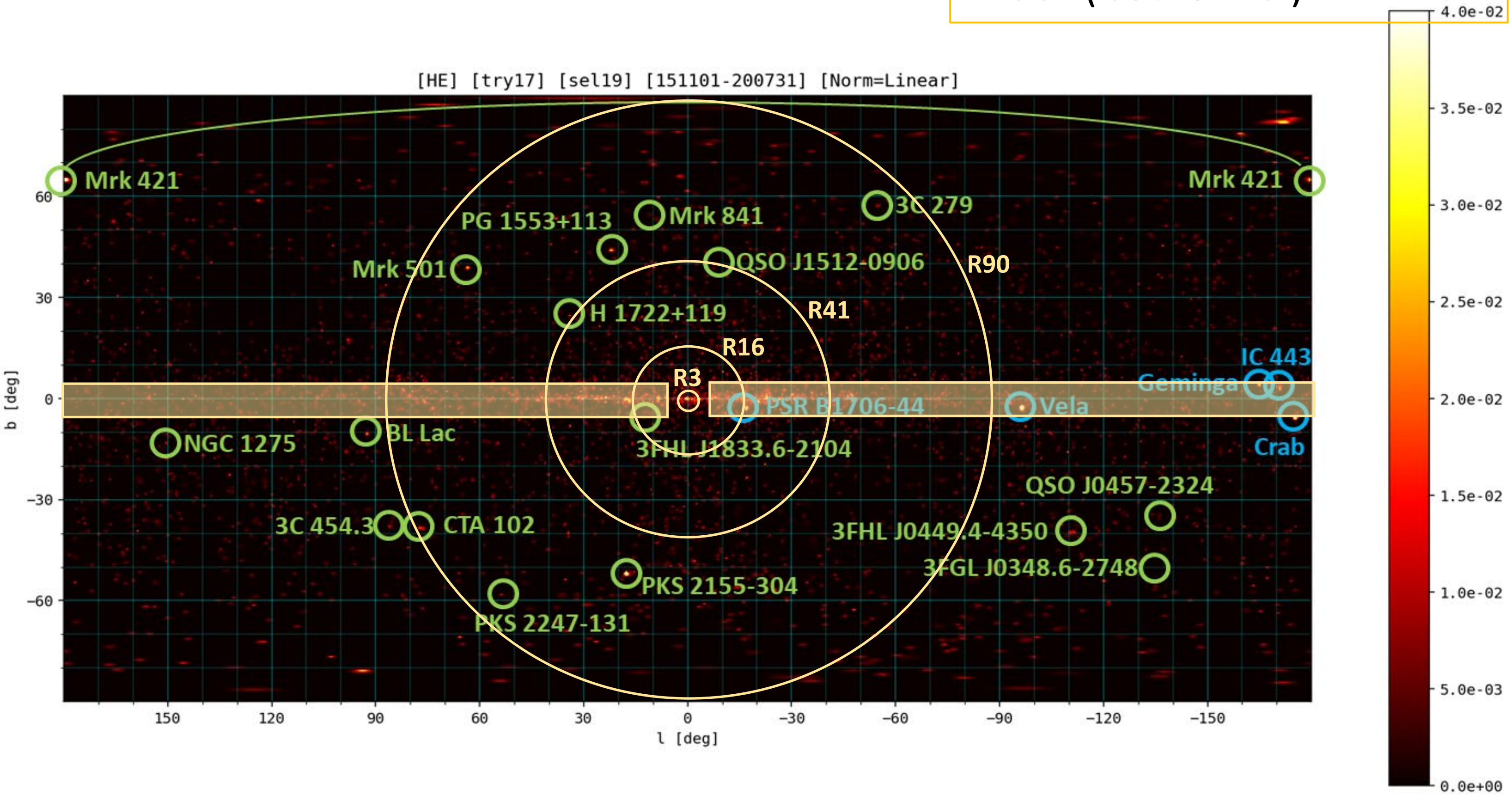

- Radius of ROI are optimized for each Galactic halo density profile model
- The disk regions ($|l|>6°$ and $|b|<5°$) and point sources are removed from analysis.

Ackermann+, PR D91, 122002 (2015)

Dark matter density profile

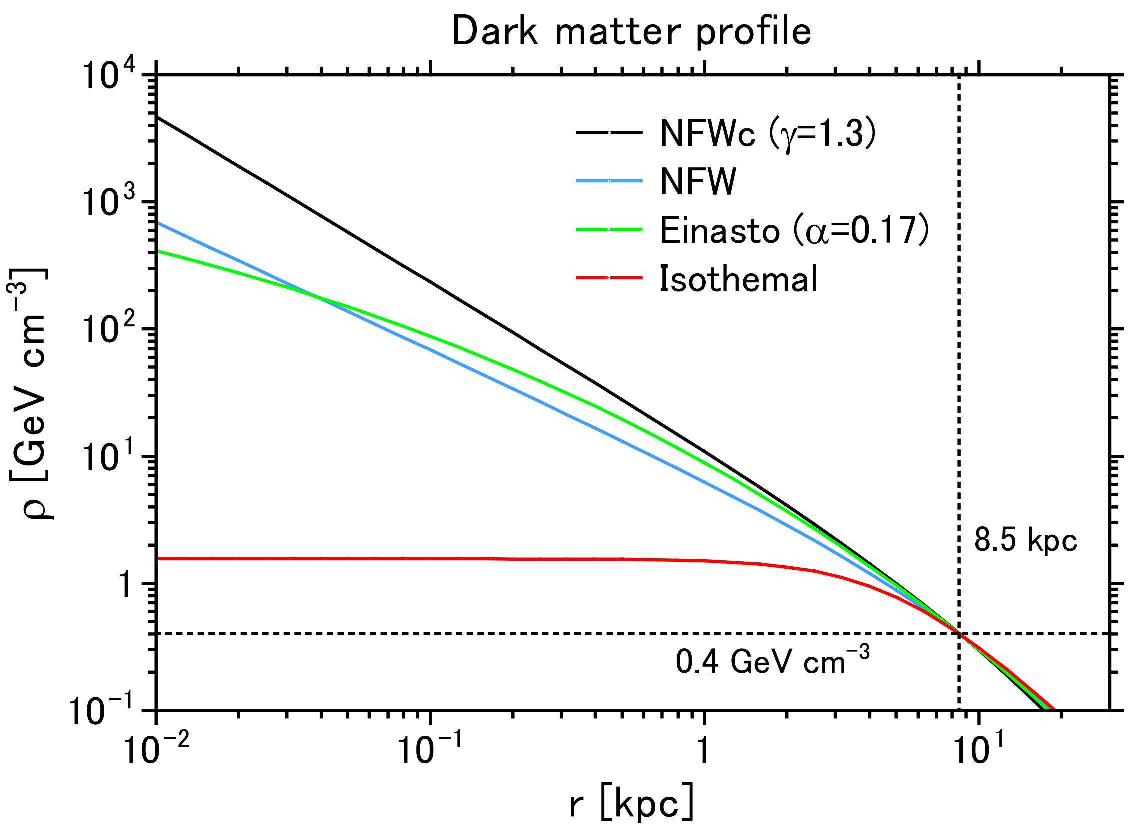

- Normalized to be 0.4 GeV cm^{-3} at 8.5 kpc from the Galactic center.
- Different densities are predicted around the Galactic center.

Line-of-sight profile

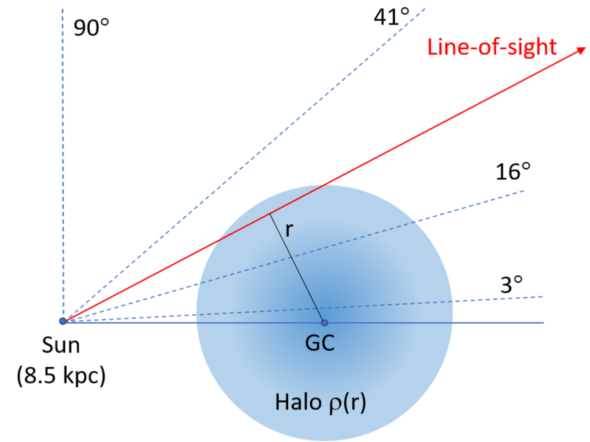

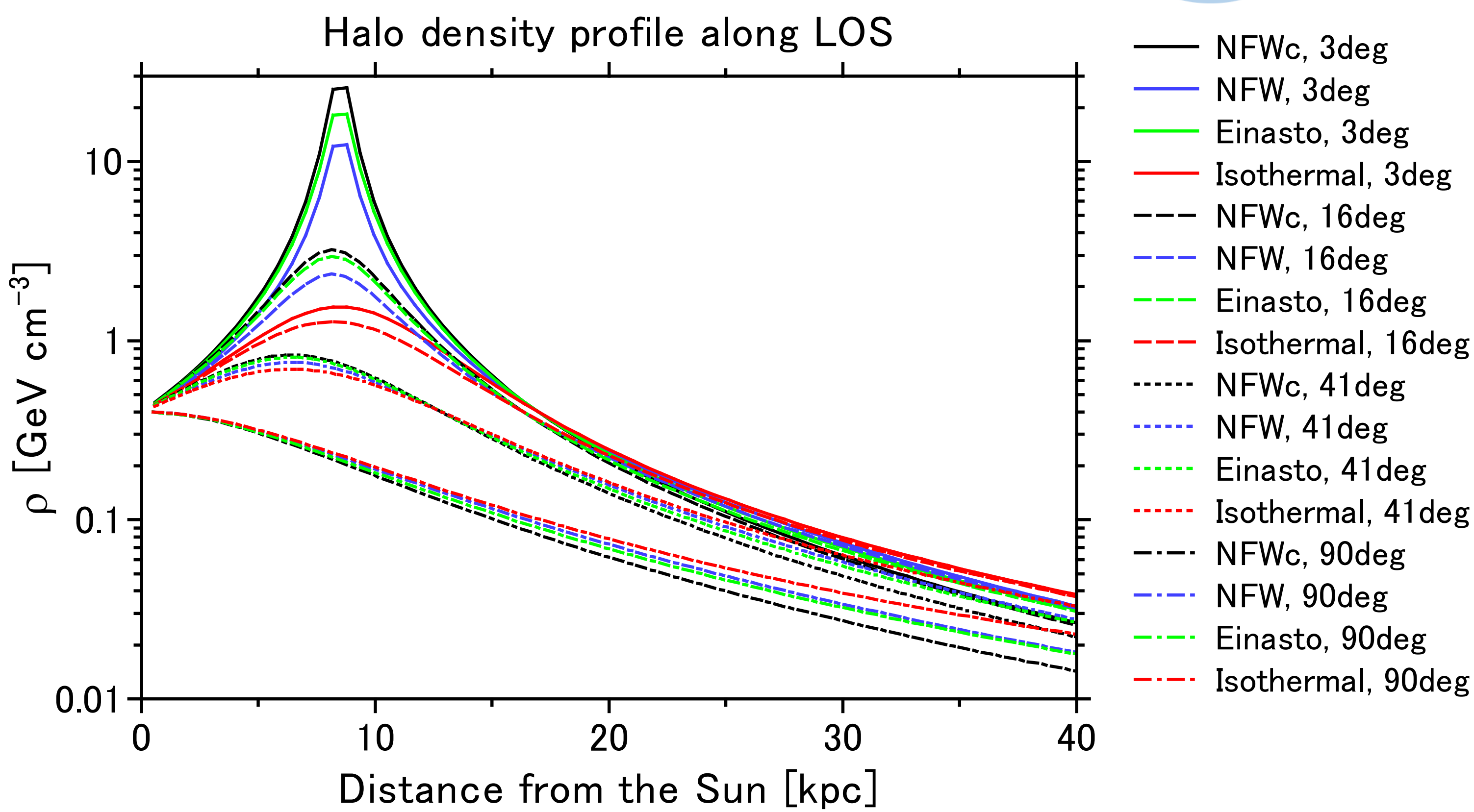

- We expect larger signals toward the Galactic center for cuspy profiles.

Calculation of upper limits

- Monoenergetic lines are assumed.
- Adding the assumed line signals (broadened by a Gaussian distribution with CALET energy resolution) to the observed spectra which raise the reduced χ^2 for the power-law fit by 3.94 (corresponding to 95% C.L.).

R16: E_{DM} = 39.8 GeV case

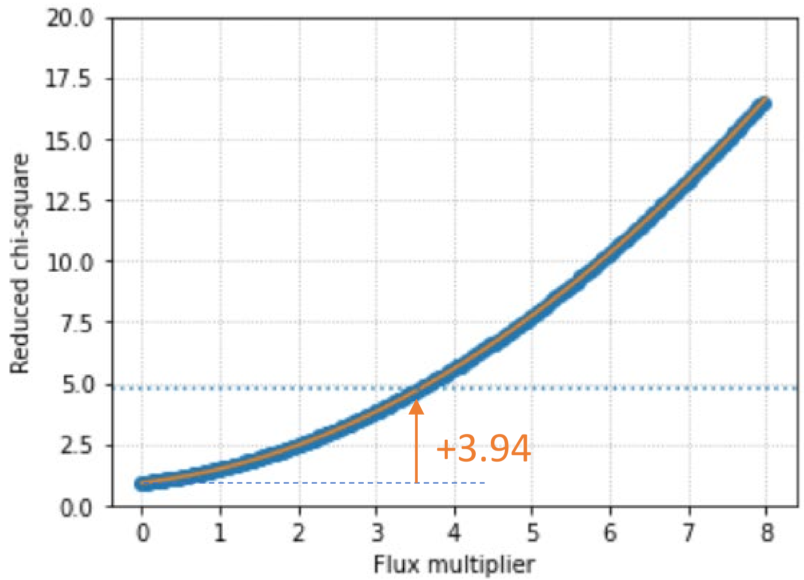

Assumed flux (unit: Power-law-fit)

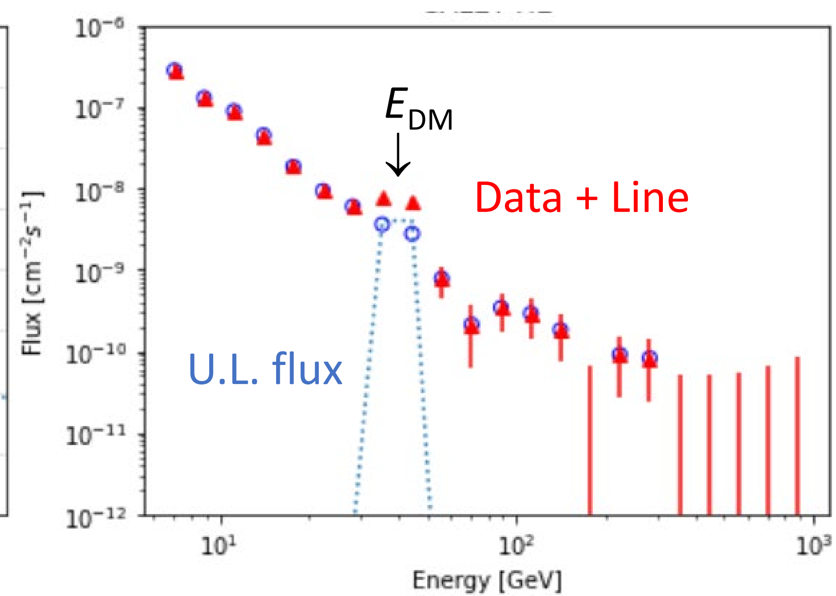

Upper limits as a function of energy

Preliminary

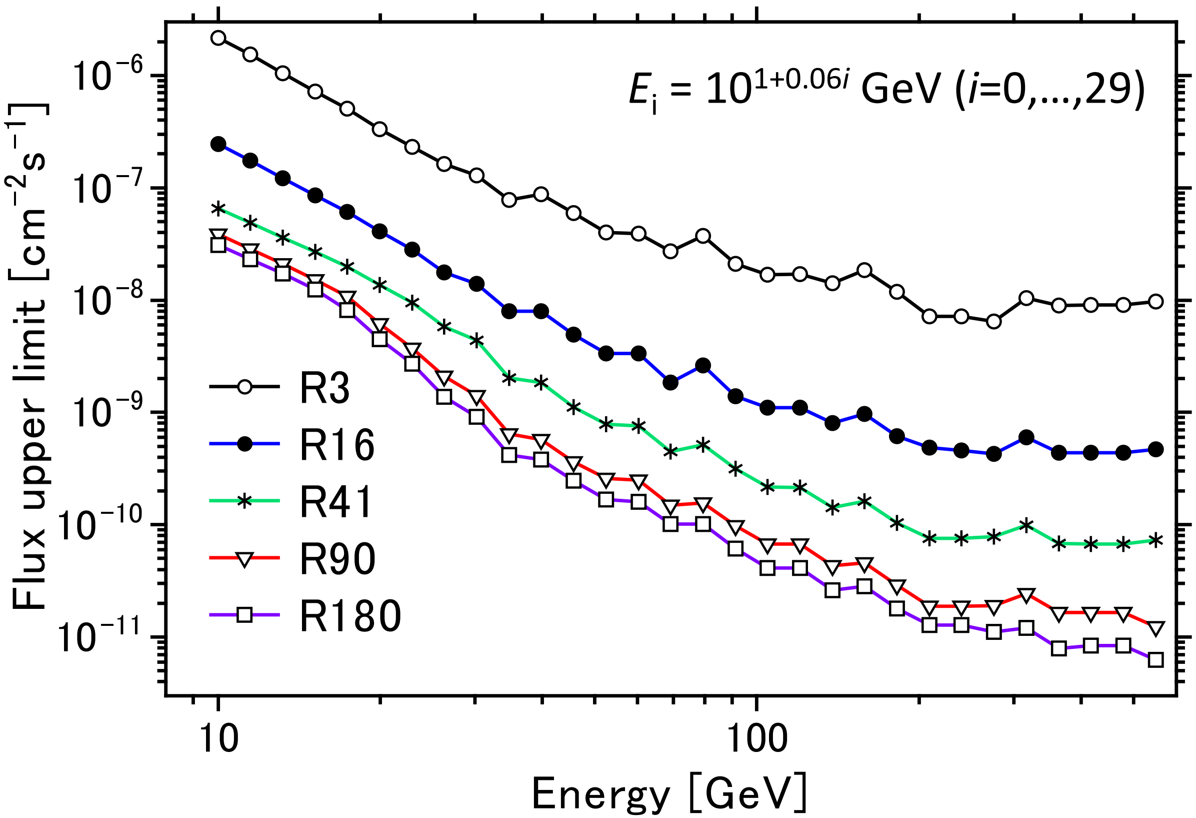

- Upper limits are mostly determined by event statistics.
- Systematic errors are not taken into account (under study).

Gamma-ray line signal from dark matter

- **Annihilation**

$$\left(\frac{\mathrm{d}\Phi}{\mathrm{d}E}\right)_{\mathrm{ann}} = \frac{\langle\sigma v\rangle}{8\pi m_{\mathrm{DM}}^2}\left(\frac{\mathrm{d}N}{\mathrm{d}E}\right)_{\mathrm{ann}}\left[\int_{\mathrm{ROI}} \mathrm{d}\Omega \int_{\mathrm{l.o.s.}} \mathrm{d}s\,\rho(r)^2\right]$$

$<\sigma v>$: velocity-averaged cross section

$\mathrm{d}N/\mathrm{d}E = 2\delta(E_\gamma - E)$, $E_\gamma = m_{\mathrm{DM}}$

- **Decay**

$$\left(\frac{\mathrm{d}\Phi}{\mathrm{d}E}\right)_{\mathrm{dec}} = \frac{1}{4\pi\tau_{\mathrm{DM}} m_{\mathrm{DM}}}\left(\frac{\mathrm{d}N}{\mathrm{d}E}\right)_{\mathrm{dec}}\left[\int_{\mathrm{ROI}} \mathrm{d}\Omega \int_{\mathrm{l.o.s.}} \mathrm{d}s\,\rho(r)\right]$$

τ_{DM}: lifetime

$\mathrm{d}N/\mathrm{d}E = \delta(E_\gamma - E)$, $E_\gamma = m_{\mathrm{DM}}/2$

J-factors: $\left[\int_{\mathrm{ROI}} \mathrm{d}\Omega \int_{\mathrm{l.o.s.}} \mathrm{d}s\,\rho(r)^2\right]$, $\left[\int_{\mathrm{ROI}} \mathrm{d}\Omega \int_{\mathrm{l.o.s.}} \mathrm{d}s\,\rho(r)\right]$ halo-model dependent!

Integral of (halo density)^2 $\rho(\underline{r})^2$ [halo density $\rho(\underline{r})$] along line-of-sight (l.o.s.) over Region-of-Interest (ROI)

Fermi-LAT: Ackermann+, PR D91, 122002 (2015)
H.E.S.S.: Abdallah+, PRL 120, 201101 (2018)

Upper limits on <σv>

Thin line: thermal relic ($3\times10^{-26}\,\mathrm{cm^3s^{-1}}$)

Preliminary: statistical error only

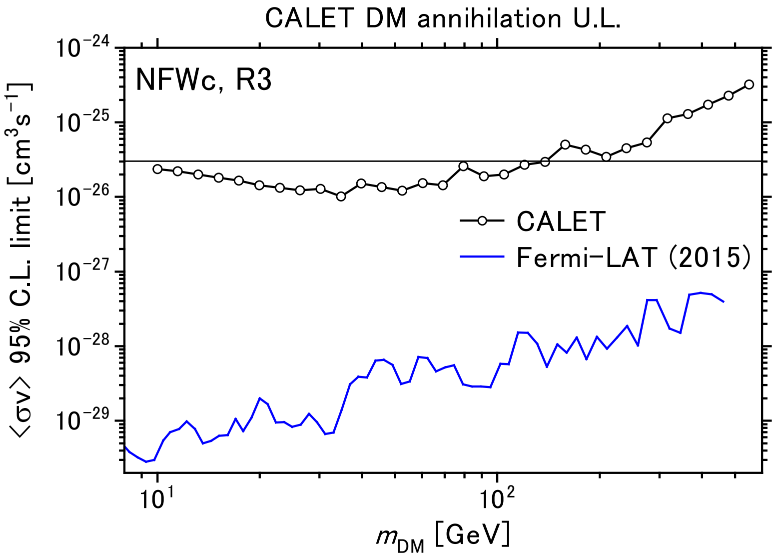

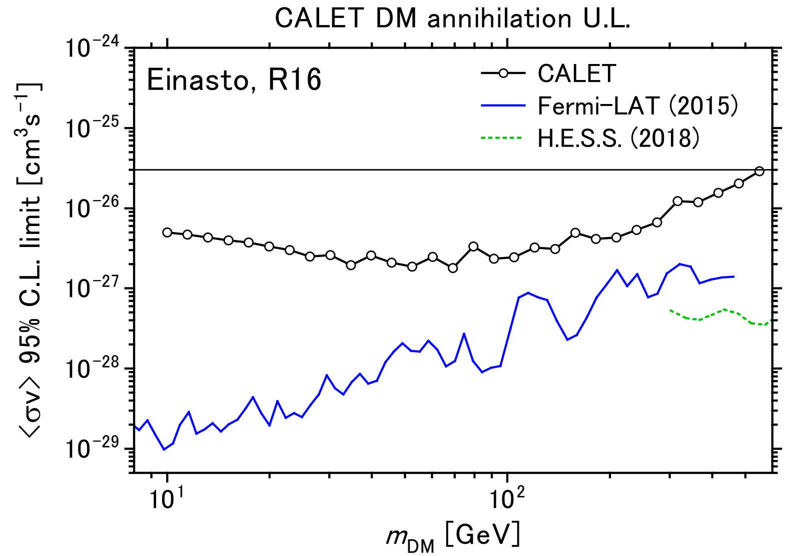

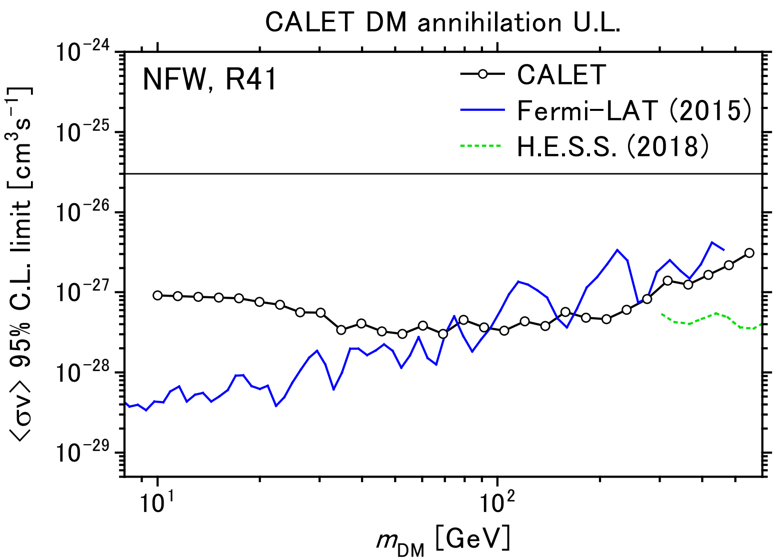

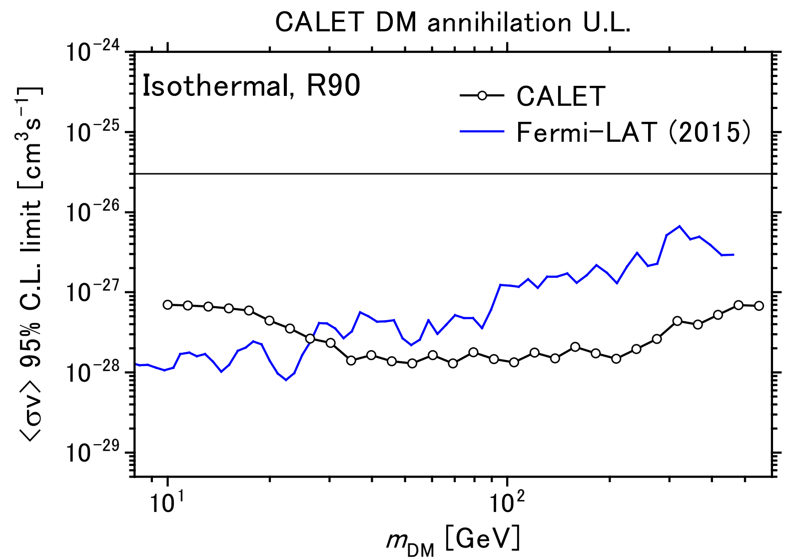

Fermi-LAT: Ackermann+, PR D91, 122002 (2015)

Upper limits on lifetime

Preliminary: statistical error only

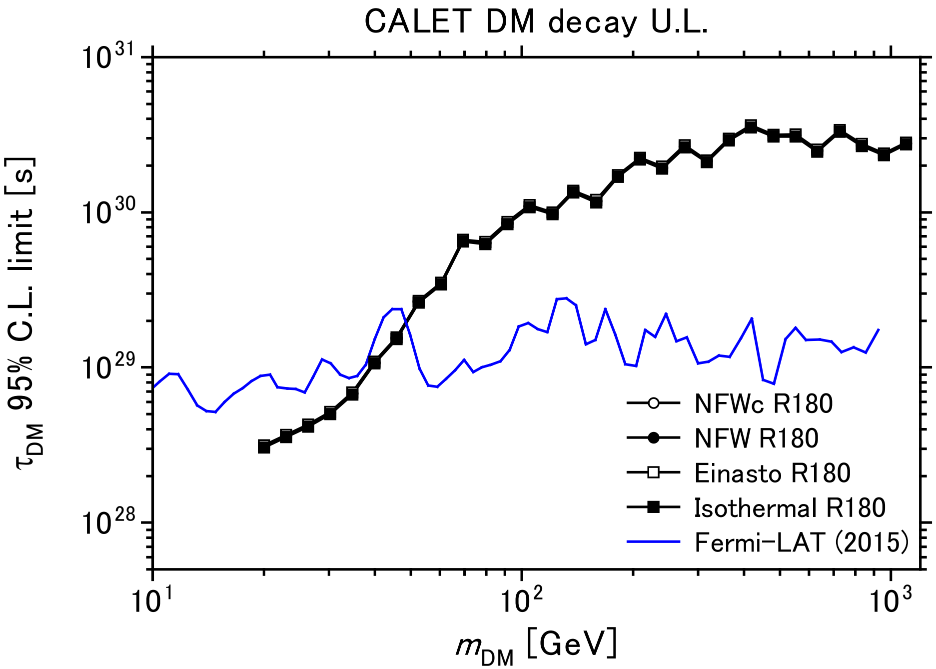

For R180, limits are almost independent of the profile models.

- Good energy resolution of CALET enables sensitive search at high energies, but limited by the statistics of observed gamma rays.
- Thus for larger ROI, we may set better upper limits.

Summary

- Gamma-ray events above 10 GeV observed during five years of operation of the CALET detector have been analyzed to search for possible line signals.
- Good energy resolution of CALET enables sensitive search in the high energy region.
- We found no hint of line signals and gave upper limits on parameters of the DM annihilation and decay models for $m_{DM} = 10 \sim 500$ GeV.
- For annihilation, $\langle\sigma v\rangle_{\gamma\gamma} < 10^{-28}\text{-}10^{-25}\mathrm{cm}^{-3}\mathrm{s}^{-1}$ depending on m_{DM} and the Galactic halo density models.
- For decay, lifetime limits reach $\tau_{DM} > 10^{30}$s (m_{DM}>100 GeV) and almost model-independent.
- We are now studying possible systematic errors in our limits.

See also PoS (ICRC2021) 619